13A.3 USING SHORT RANGE ENSEMBLE FORECASTS AND HIGH RESOLUTION MODEL GUIDANCE TO ASSESS THE POTENTIAL FOR TORNADOES ACROSS SOUTHEAST VIRGINIA ON 28 APRIL 2008

Josh Korotky
NOAA/NWS, Pittsburgh, PA
and
Richard H. Grumm
NOAA/NWS, State College, PA

1. INTRODUCTION

Short Range Ensemble Forecast (SREF) system (Du et al. 2006) products are used with high resolution model output to identify the potential for supercells and tornadoes across southeast Virginia on 28 April 2008. This study will demonstrate that SREF probability forecasts and high resolution deterministic model output shouldn't be considered as mutually exclusive approaches to forecasting. Rather, the complementary strengths of both approaches can lead a forecaster to greater situational awareness for a high impact event (Korotky 2006, Weiss et al. 2006, Roebber et al. 2004).

The tornado outbreak across southeast Virginia during the late afternoon and evening hours of 28 April resulted in 10 tornadoes and multiple injuries, including an EF3 rated tornado in the city of Suffolk, VA. Figure 1 shows the Hydrologic Prediction Center (HPC) subjective surface analysis valid 1800 UTC on 28 April, and a tornado map from the Weather Forecast Office (WFO AKQ) in Wakefield VA (bottom). The figure depicts a pre-frontal squall line in the warm sector ahead of an advancing cold front.

Although clouds ahead of an advancing cold front were expected to limit destabilization across the mid-Atlantic region, this study will show that persistent low-level moisture inflow coupled with increasing low- to mid-level wind fields provided sufficient vertical wind shear to increase the potential for supercells and bowing line segments along the pre-frontal trough.

This study demonstrates a forecast strategy that uses SREF output to assess the potential for supercells and tornadoes, SREF climate anomalies to evaluate the climatological context of the model forecasts, and high resolution model output to resolve the mesoscale organization and evolution of deep convection.

Corresponding author address: Josh Korotky, NOAA/NWS, 192 Shafer Rd., Coraopolis PA 15108
E-mail: josh.korotky@noaa.gov

2. DATA

Forecast Tools from the SPC include SREF output, Interactive Plumes, and Mesoanalysis Graphics. Output from the 4 km NCEP Nonhydrostatic Mesoscale Model (NMM) Weather Research and Forecasting (WRF) Model includes the Simulated radar Reflectivity Factor (SRF) and 2-5 km Updraft Helicity (UH, Kain et al 2008). Standardized anomalies (SAs), displayed as a standard deviation from normal (SDs), were created from re-analysis climatological data from the NCEP/NCAR global re-analysis project (Kalnay et al. 1996). SAs are applied to NAM-WRF and SREF model output (Hart and Grumm 2001, Grumm and Hart 2001) and analyzed for the event.

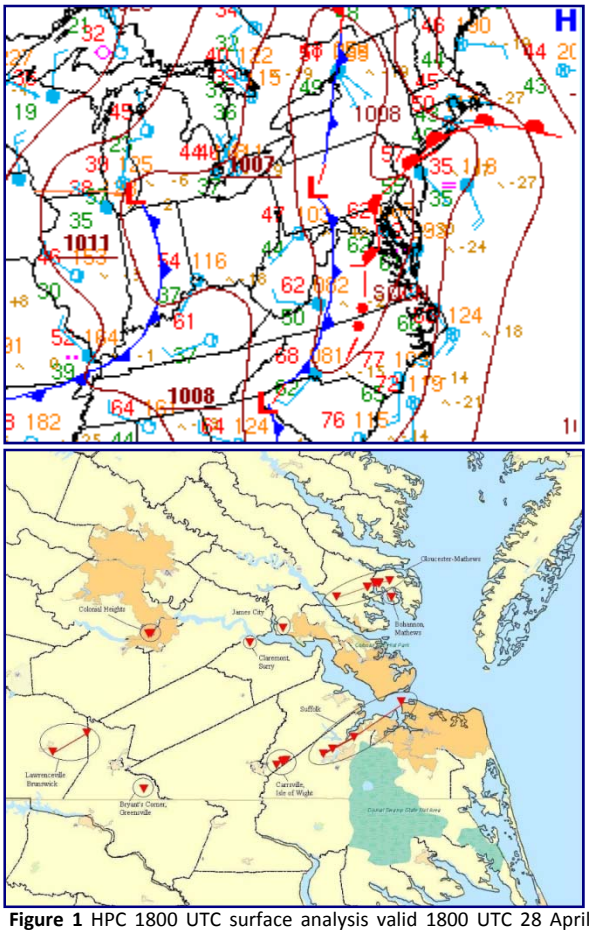

Figure 1 HPC 1800 UTC surface analysis valid 1800 UTC 28 April 2008 (top) and SPC Tornado Reports (bottom).

3. MODEL/SREF/CLIMATE ANOMALY FORECASTS

Operational NAM, SREF, and climate anomaly forecasts are used to assess the pre-storm environment on 28 April, including the potential for supercells and tornadoes. A 3-hr forecast of SREF ensemble mean precipitable water (PW, top) and 2m dew points (Td, bottom), valid 1800 UTC 28 April, depicts PW values near 1.5 in. across southeast VA with corresponding Tds in the low to mid 60s (Fig. 2).

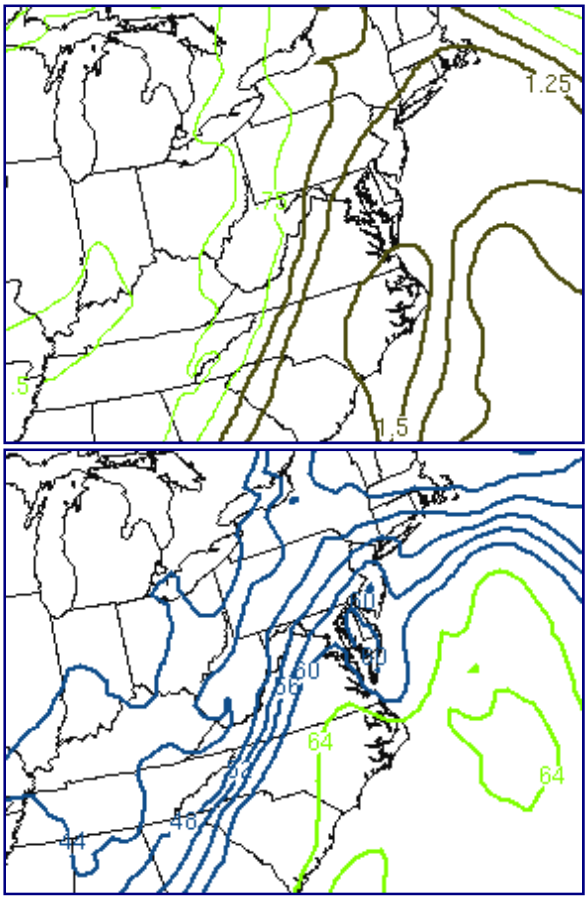

Figure 2 SREF ensemble mean precipitable water (in, top) and 2m dew points (°F, bottom) initialized at 1500 UTC 28 April and valid 1800 UTC 28 April.

Figure 3 depicts NAM 00-hr forecasts valid 1800 UTC 28 April of 850 hPa winds (kts) and 850 hPa v-wind anomalies (top). Precipitable water (mm) and precipitable water anomalies are displayed in the bottom panel. 850 hPa wind anomalies in the warm sector are between +2 and +3 SDs, and PW departures from climatology are between +1 and +2 SDs across southeast VA. These anomalies indicate that the low level jet is forecast to be a significant factor in the storm environment, especially when paired with a forecast of above normal moisture.

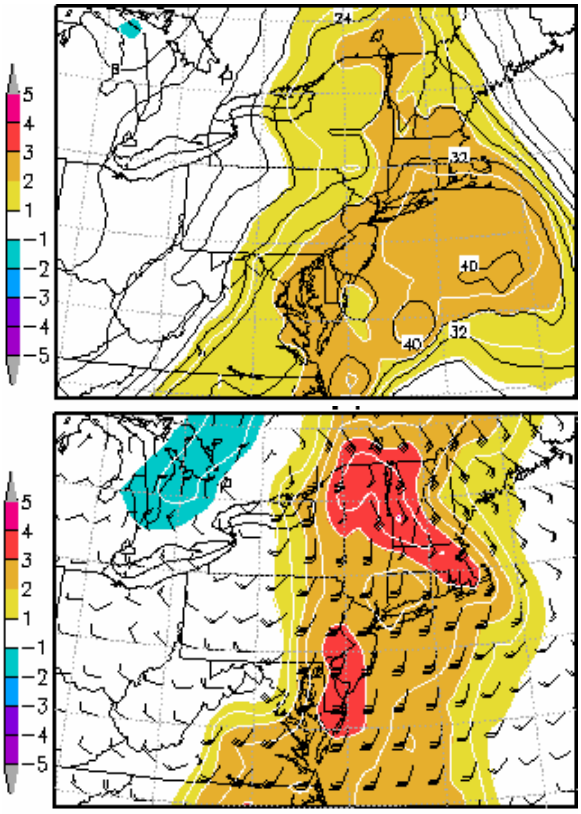

Figure 3 NAM 850 hPa winds (kts) and 850 hPa v-wind anomalies (top); precipitable water (mm) and precipitable water anomalies (bottom) from the 00-hour forecast, valid 1800 UTC 28 April 2008.

Figure 4 shows the NAM low, mid, and high cloud cover (top) and probability of the MLLCL < 750 m AGL (bottom), valid 1800 UTC 28 April. The SREF 100 mb mean LCL = 750 m is depicted with a black dashed contour (bottom). The top panel of Figure 4 shows that low clouds are forecast to prevail over SE VA at 1800 UTC, and the bottom panel indicates that Lifting Condensation Level (LCL) heights will likely (~ 90% probability) be less than 750 m AGL across the region. Edwards and Thompson (2000) found that the LCL height discriminates strongly between significantly tornadic (F2-F5) and nontornadic supercells, and established that no strong or violent tornadoes occurred for LCLs > 1500 m AGL. Thompson et al. 2003 substantiated the findings of Edwards and Thompson (2000), and determined that LCL heights below roughly 1000 m AGL were meteorologically significant for discriminating between significantly tornadic and nontornadic supercells. Markowski et al. (2002) found that relatively warm, moist, and potentially buoyant Rear Flank Downdraft (RFD) air is most likely a requirement for the development of significant (F2-F5) tornadoes, and suggested that environments with high boundary layer relative humidity (and low cloud bases) appear to favor potentially buoyant RFDs. Figure 4

therefore indicates that the environment might support tornadoes if CAPE and vertical wind shear measures favor supercell development.

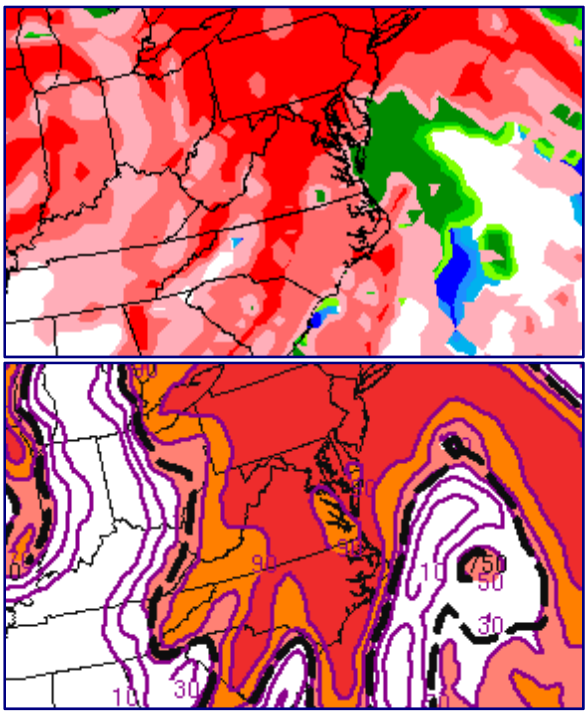

Figure 4 Top: NAM low clouds (red), mid clouds (green), and high clouds (blue). Darker shades = higher %. Bottom: probability MLLCL < 750 m (fill) and SREF mean 100 mb MLLCL = 750 m (black-dashed).

One of the strengths of an Ensemble Prediction System (EPS) is the ability to calculate and display probabilistic forecasts. Figure 5 (top) shows the NAM Effective Bulk Shear (EBS). Fig 5 (bottom) shows an interactive plume chart, depicting the SREF uncalibrated probability of EBS exceeding 30 kts (blue), 40 kts (red), and 50 kts (black) over time. SREF probabilities represent the relative frequency of EPS members forecasting a common occurrence of some diagnostic variable (e.g., EBS > 40 kts) at a grid point divided by the total number of EPS members. EBS (Thompson et al. 2004) is similar to the 0-6 km bulk shear, but it accounts for storm depth (effective inflow base to EL) and is designed to identify the potential for both surface-based and elevated supercells. Supercells become increasingly likely when the EBS increases in magnitude to a range of 25-40 kts and greater. Figure 5 (top) shows NAM EBS magnitudes around 40 kts in the warm sector across SE VA at 1800 UTC. Figure 5 (bottom) indicates a 95% probability of EBS > 30 kts, a 62% probability of EBS > 40 kts, and a 14% probability of EBS > 45 kts. The figure illustrates that EBS will likely be in a range to support supercells.

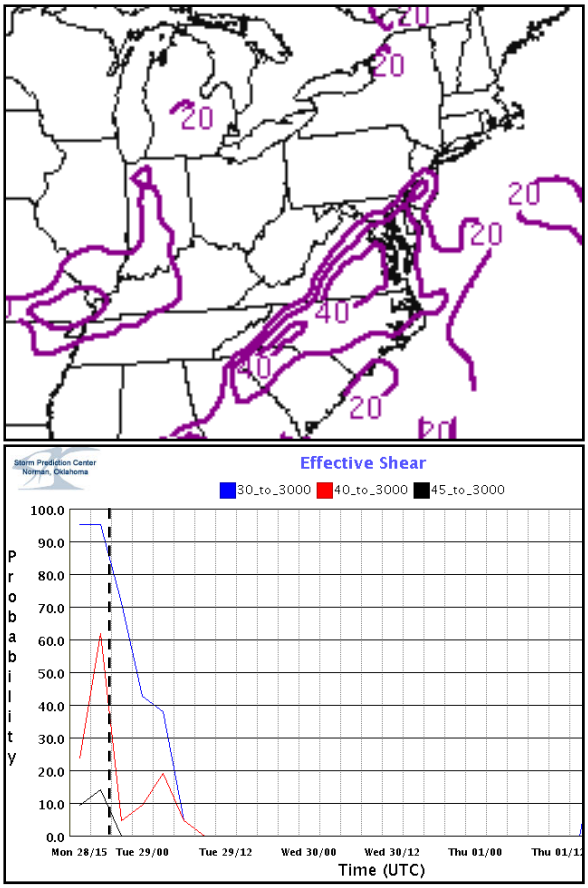

Figure 5 NAM-WRF EBS (top); SREF probability of EBS exceeding 30 kts (blue), 40 kts (red), and 50 kts (bottom). The dashed line represents 1800 UTC.

Figure 6 shows the NAM-WRF Most Unstable CAPE (MUCAPE, top), valid 1800 UTC, and an interactive plume chart (bottom) depicting the SREF probabilities of MUCAPE exceeding 500 Jkg^{-1}, 750 Jkg^{-1}, and 1000 Jkg^{-1} over time. The MUCAPE is forecast to be around 500 Jkg^{-1} across SE VA, a value substantiated by SREF probabilities, which indicate that 500 Jkg^{-1} will be the most likely category (~ 62%, bottom).

EPS also permits the computation of combined probabilities (CBs), defined as the product of individual probabilities. The top panel of Figure 7 shows the SREF combined probability of convective precipitation (CP) exceeding .01 in, MUCAPE exceeding 500 Jkg^{-1}, and EBS exceeding 40 kts. The bottom panel shows an interactive plume chart depicting the SREF probability of MUCAPE exceeding 500 Jkg^{-1}, EBS exceeding 40 kts, and the CB of MUCAPE exceeding 500 Jkg^{-1} and EBS exceeding 40 kts (bottom) over time. These data indicate a 40-50% probability of receiving CP in an environment which also supports MUCAPE > 500 Jkg^{-1} and EBS > 40 kts. When considering CBs involving three

diagnostic variables, values in the range of 40-50% and greater are significant, especially given that they are constrained by the occurrence of CP, which isn't always handled well in the model. The interactive plumes (Fig. 7, bottom) are similar to the top panel, except the MUCAPE and EBS are not constrained by CP. Without CP the probability of jointly observing MUCAPE > 500 Jkg^{-1} and EBS > 40 kts increases to 50%.

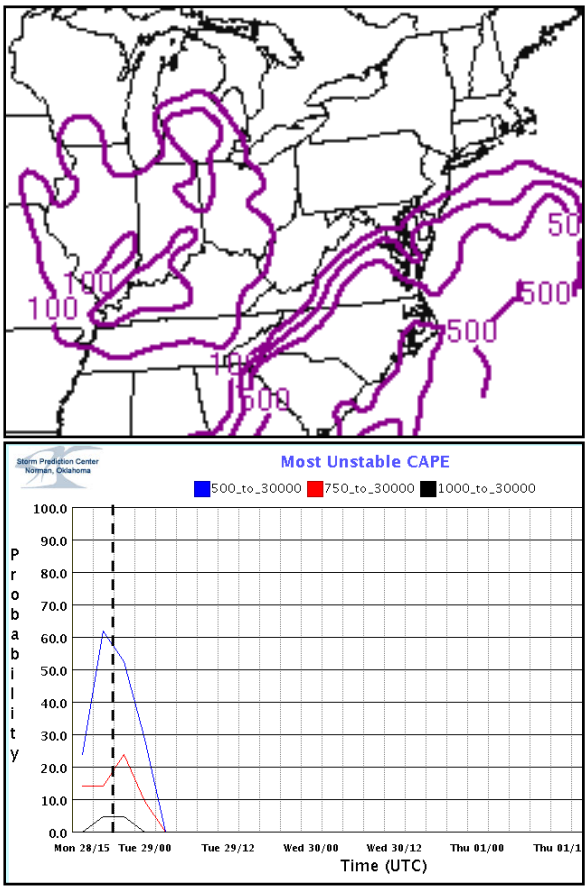

Figure 6 NAM –WRF MUCAPE (top); SREF probability of MUCAPE exceeding 500 Jkg^{-1}, 750 Jkg^{-1}, and 1000 Jkg^{-1} (bottom).

Figure 8 shows the SREF probability of 0-1km AGL Storm Relative Helicity (SRH) exceeding 150 m^2s^{-2} (top), and SREF ensemble median SRH (solid contours), union (≥ 1 member, red), and intersection (all members, blue), valid 1800 UTCl. The top panel indicates a 50-70% probability of 0-1 km SRH values > 150 m^2s^{-2} across SE VA, with an EPS mean of 150 $m^2s^{-2}$and an EPS median exceeding 150 m^2s^{-2}(bottom). SRH indicates the potential for cyclonic updraft rotation in right-moving supercells, and is calculated for the lowest 1-km and 3-km layers AGL. Although there is no clear threshold value for SRH when forecasting supercells (the formation of supercells appears to be related more significantly to deeper layer vertical shear), Edwards and Thompson (2000) found that the 0-1 km layer accounted for most of the distinction in SRH between significant tornadoes and weakly tornadic supercells. Thompson et al. (2003) indicated that the combined effects of low-level shear (e.g., 0–1 km SRH) and low-level moisture can strongly discriminate between significantly tornadic (F2-F5 damage) and nontornadic supercells. In their study 81% of the significantly tornadic supercells were associated with 0-1 km mean RH > 65% and 0–1 km SRH > 75 $m^2 s^{-2}$, while 70% of the nontornadic supercells occurred with lesser values of either parameter. For this case the predicted 0-1km SRH was > 150 $m^2 s^{-2}$, and the low level mean RH was > 80% (Figure 15).

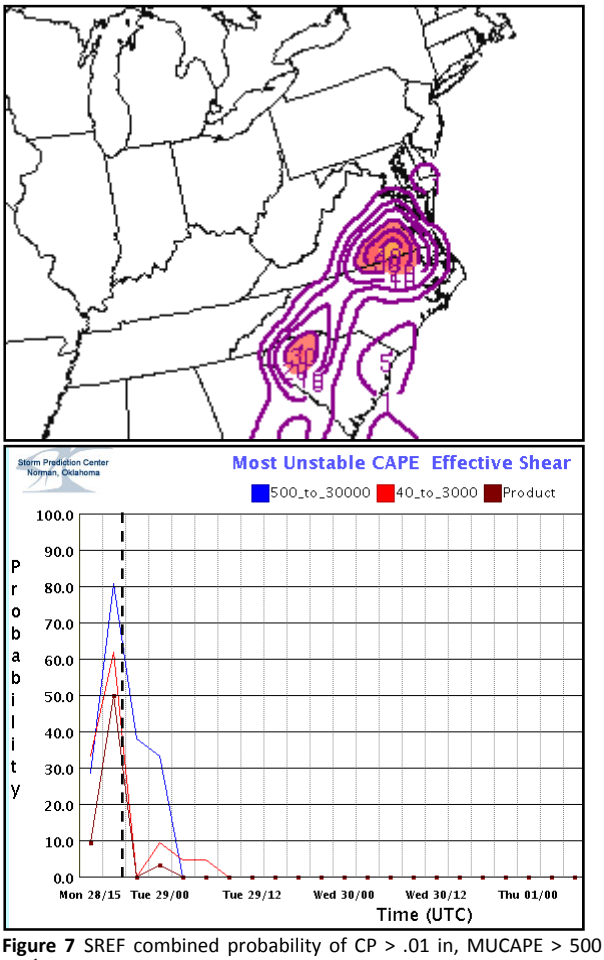

Figure 7 SREF combined probability of CP > .01 in, MUCAPE > 500 Jkg^{-1}, and EBS > 40 kts. (top) The bottom panel shows an interactive plume chart depicting the SREF probability of MUCAPE > 500 Jkg^{-1}, EBS > 40 kts, and the combined probability of MUCAPE > 500 Jkg^{-1} and EBS > 40 kts. The dashed line represents 1800 UTC.

Figure 9 shows the SREF Probability of a STP > 1 (top) and the SREF mean Supercell Composite Parameter (SCP, black) and the probability of a SCP > 1 (bottom), valid 1800 UTC. The SCP is a composite index

that includes MUCAPE, EBS, and effective SRH (ESRH, Thompson et al. 2007). Larger values of SCP indicate greater overlap in the three supercell ingredients, and discriminate strongly between surface-based supercells and discrete nonsupercells. The STP (Thompson et al. 2007) is a composite index that includes Mixed Layer CAPE (MLCAPE), EBS, ESRH, Mixed Layer LCL (MLLCL), and Mixed Layer CIN (MLCIN). Figure 9 indicates less than 10% of the SREF members depict a STP > 1 across SE VA at 1800 UTC 28 April (top), but more than 70% of the SREF members indicate a SCP > 1 (bottom). It should be noted that a 10% probability of the STP exceeding 1 can be a significant signal, given the number of terms in the STP calculation.

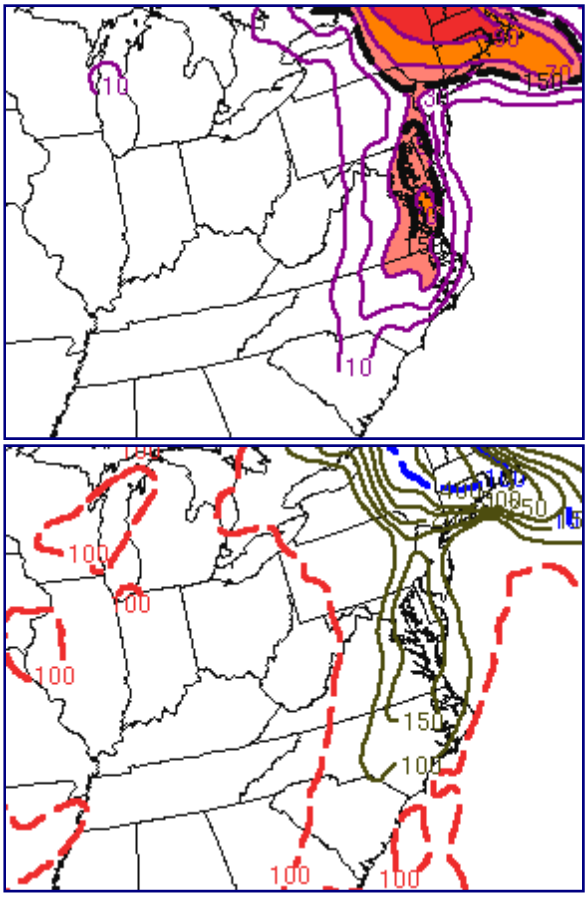

Figure 8 SREF probability of 0-1km AGL Storm Relative Helicity (SRH) exceeding 150 m^2s^{-2} (top), and SREF ensemble median SRH (solid contours), union (≥ 1 member, red), and intersection (all members, blue), valid 1800 UTC 28 April.

4. HIGH RESOLUTION MODEL OUTPUT

One of the most important goals when forecasting the potential for a high impact convective event is to correctly anticipate whether supercells and tornadoes are favored, or if the primary threat will be from bowing line segments and straight-line winds (or both). High resolution model output is particularly well suited to provide details of the mesoscale organization and evolution of deep convection, so post processed data (SRF and 2-5 km UH) from the 4 km NCEP NMM WRF were used in this study.

Figure 10 depicts 2-5 km AGL UH (top), and SRF (dBZ, bottom) from the NCEP 4 km convection allowing NMM WRF, valid 2000 UTC. UH is computed directly in the model, and represents a 2-5 km integration of the product of vertical motion and the vertical component of relative vorticity (Kain et al. 2008). In a study based on data from the 2005 NOAA HWT Spring Experiment, Kain et al. (2008) showed that UH could be used as a substitute for supercells in model forecasts. The HWT Spring Experiment demonstrated that the 4 km Advanced Research WRF (ARW) generated storms with UH maxima (mesocyclones) in environments that produced observed supercells.

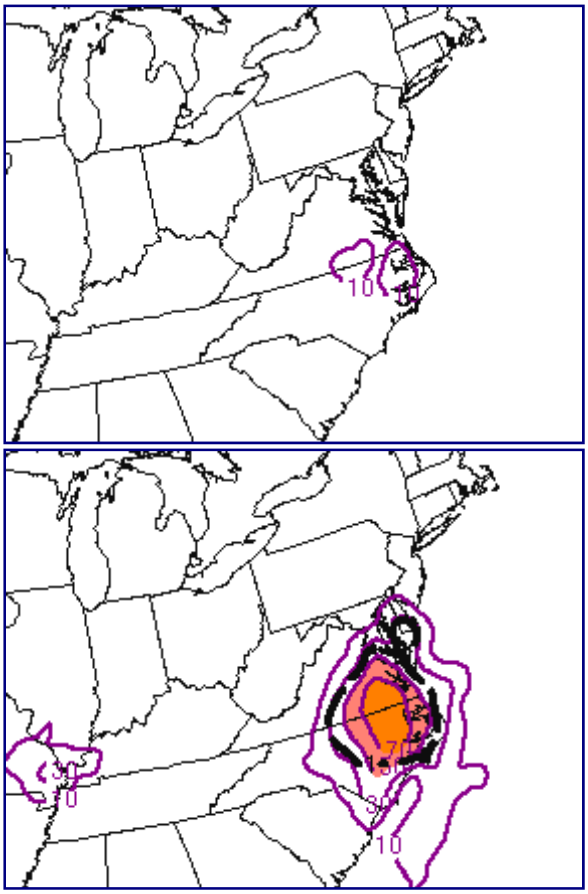

Figure 9 SREF Probability of the STP > 1 (top); SREF mean SCP (black) and probability of the SCP > 1 (bottom), valid 1800.

The SRF is based on the model forecast of precipitation-sized hydrometeors. Koch et al. 2005 established that the SRF can provide an effective way to forecast the intensity, movement, and coverage of precipitation features. Figure 9 indicates UH (top panel) associated with cellular elements ahead of bowing line segments (bottom panel) across SE VA. UH values across SE VA at 2000 UTC range from 8 to 12 m^2s^2. While specific details of storm placement and character do not exactly match, the WRF-NMM accurately predicted the primary region of supercell development. In many cases where forcing is strong, a juxtaposition of SRF and UH can highlight supercell and tornado potential, especially when used with other diagnostic approaches that reveal the magnitude/coverage of moisture, instability, vertical wind shear, and sources of lift/lifting mechanisms.

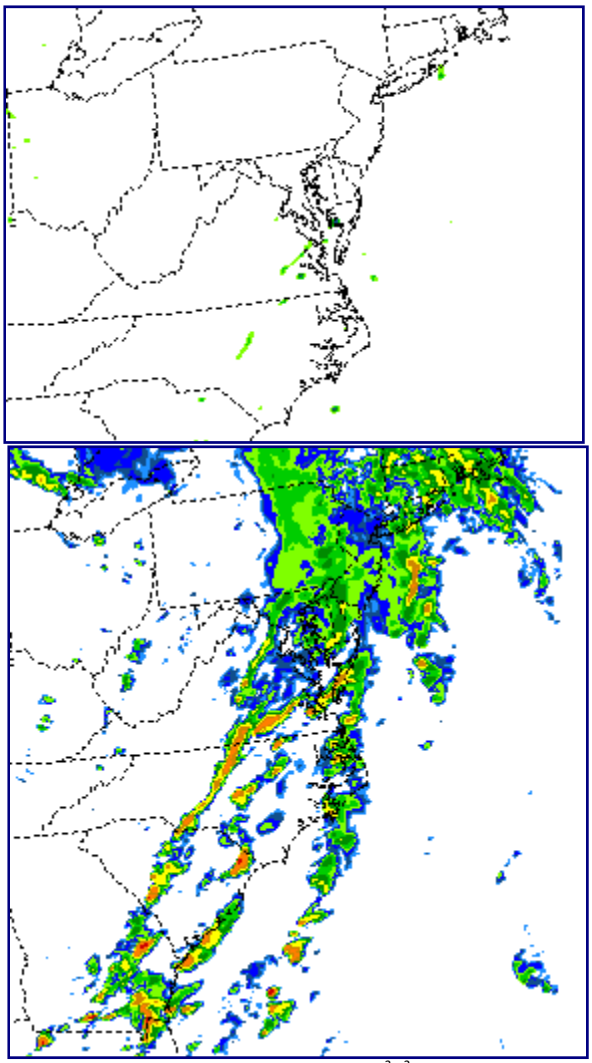

Figure 10 2-5 km AGL Updraft Helicity (m^2s^{-2}, top), and Simulated Radar Reflectivity (dBZ) from the NCEP 4 km NMM WRF (bottom), valid at 2000 UTC 28 April.

Figure 11 shows the 0.5° Base Reflectivity (BREF) from the Norfolk VA/Wakefield (KAQC) WSR-88D valid 1900 UTC 28 April. When comparing Figure 10 and Figure 11, the similarity between the SRF and BREF is striking, especially given the model development of cellular elements containing UH maxima (mesocyclones).

Figure 12 illustrates the NAM-WRF 3-hr. convective precipitation (CP) forecast, ending 2100 UTC 28 April. Maximum values of CP range from 0.3 to 0.4 in. (blue fill) across parts of S and SE VA. Although not as detailed in placement and timing as the SRF, the CP maximum appears to highlight the supercell potential. This is a valid assumption because all of the previous diagnostics (e.g., EBS, SCP, probability/joint probability graphics, SRF/UH) point to an enhanced potential for supercells across SE VA during the late afternoon.

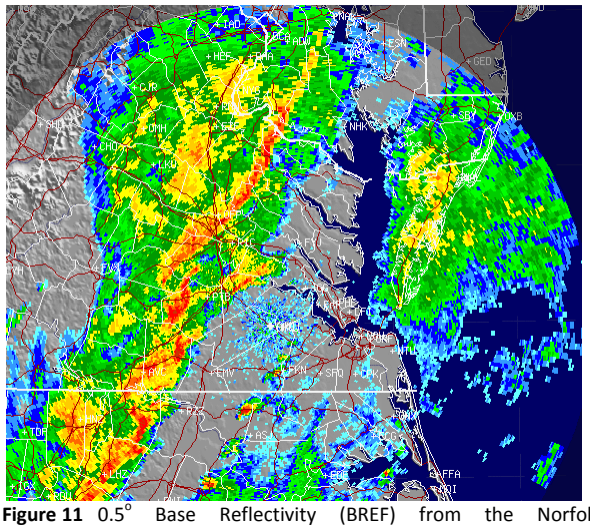

Figure 11 0.5° Base Reflectivity (BREF) from the Norfolk VA/Wakefield (KAKQ) WSR-88D valid 1900 UTC 28 April.

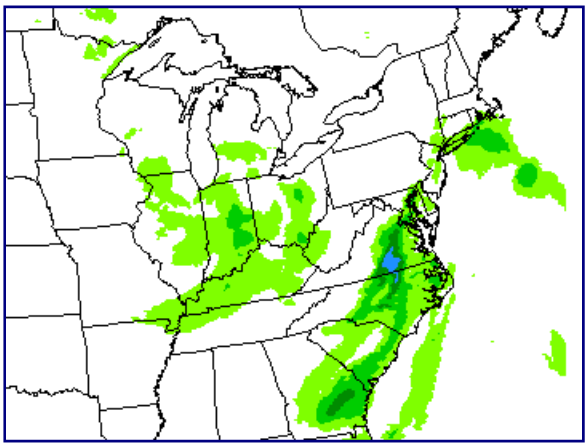

Figure 12 NAM 3-hr convective precipitation (in.) valid 1800-2100 UTC 28 April, initialized at 1200 UTC 28 April.

5. MESOANALYSIS GRAPHICS

SPC mesoanalysis graphics (Bothwell et al. 2002) provide an effective way to link forecasts with real time changes in the mesoscale environment. This linkage is essential for increasing situational awareness of changing severe weather potentials.

Figure 13 shows Rapid Update Cycle (RUC, Benjamin 1994) effective layer SCP (top); fixed layer STP (contours) and MLCIN (Jkg^{-1}, shaded at 25 and 100). The top panel indicates a SCP > 4 across SE VA and the bottom panel depicts a FLSTP of at least 1. Again, a FLSTP of 1 can be a significant signal given the number of terms in the calculation. The FLSTP (which replaces MLCAPE with SBCAPE, effective shear/SRH with 0-1 km SRH and 0-6 km bulk shear, and SBLCL) was used here instead of the effective layer STP because RUC soundings portrayed a consistent and erroneous dry bubble in the lowest part of the sounding, which underplayed the effective layer STP (Jon Davies, personal communication).

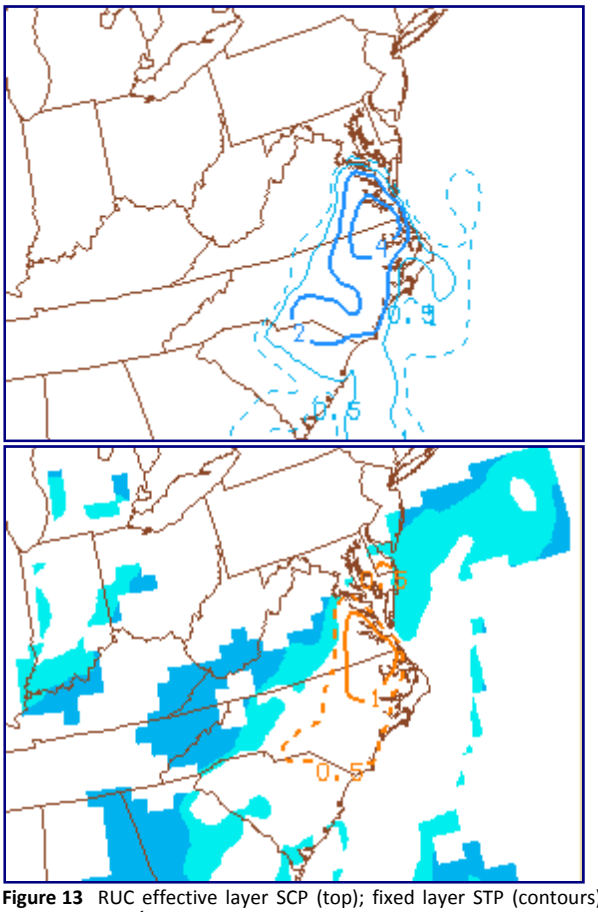

Figure 13 RUC effective layer SCP (top); fixed layer STP (contours) and MLCIN (Jkg^{-1}, shaded at 25 and 100), valid 1800 UTC 28 April.

Figure 14 shows EBS (kts, top), and the 0-1 km Energy Helicity Index (EHI, Hart and Korotky 1991) (bottom), from the RUC at 1800 UTC 28 April. The top Panel indicates an EBS of 40-45 kts across SE VA at 1800 UTC, and the bottom panel shows a 0-1 km EHI of 2 across the region. Given an SCP > 4 and a FLSTP of 1 (Figure 13), and an EBS of 40-45 kts in conjunction with a 0-1 km EHI of 2 (Figure 14), the environment appears primed for supercells across SE VA at 1800 UTC.

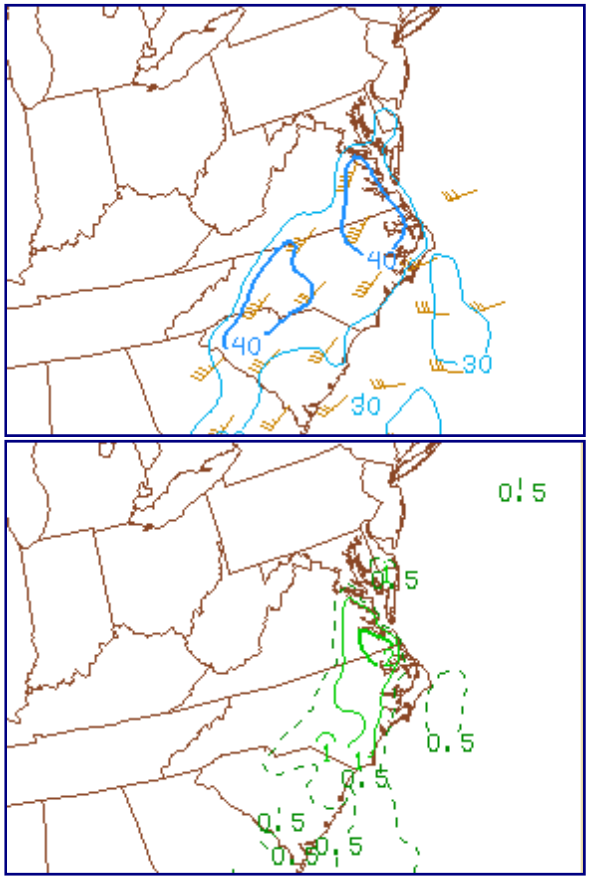

Figure 14 As in Figure 12 except EBS (kts, top) and 0-1 km EHI (bottom).

Figure 15 shows the mean RH from the LCL to the Level of Free Convection (LFC) and MUCAPE (top); the SREF mean 0-1 km SRH and SREF mean LCL heights (bottom). The figure indicates MUCAPE around 1000 Jkg^{-1}, LCL to LFC RH 80-90%, 0-1 km SRH > 200 m^2s^{-2}, and mean LCL heights < 750 m. Recalling the importance of high boundary layer RH for the production of tornadoes (Markowski et al. 2002, Thompson and Edwards 2003), a mean LCL to LFC RH of 80-90% with LCL heights < 750 is noteworthy, especially considering the MUCAPE from the RUC is considerably higher than the forecast MUCAPE of 500 Jkg^{-1}. Given a consistent forecast of supercell potential

with a small but notable possibility of tornadoes across the region, the increase in MUCAPE in conjunction with a saturated boundary layer indicate a heightened threat from supercells (and possibly tornadoes) during the afternoon. Although it would be difficult to forecast a tornado outbreak with the given information, situational awareness should dictate the possibility of a strong tornado, especially for supercells in advance of a line composed of bowing segments.

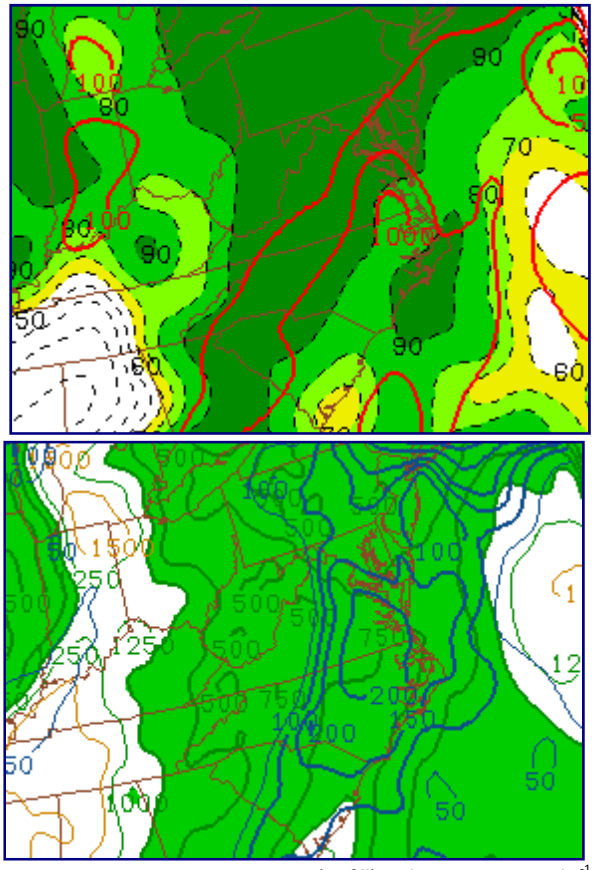

Figure 15 Top: LCL to LFC mean RH (%, fill) and MUCAPE > 100 Jkg^{-1} (red contours). Bottom: 0-1km SRH > 100 m^2s^{-2} (blue contours, every 50 m^2s^{-2}), SREF mean LCL heights (contours, m), mean LCL heights < 1000 m (shaded).

6. DISCUSSION AND CONCLUSIONS

SREF probability forecasts established a significant potential for supercells across SE VA during the late afternoon of 28 April. Characteristics of the forecast environment included EBS around 40 kts and MUCAPE roughly 500 J kg^{-1}. Other noteworthy factors included a likelihood of 0-1 km SRH > 150 m^2s^{-2} across SE VA, with a SREF ensemble mean of 150 m^2s^{-2}. SREF joint probability graphics indicated up to a 50% probability that the region would receive CP and the environment would also supported MUCAPE > 500 Jkg^{-1} and EBS > 40 kts. SREF single probability graphics indicated less than a 10% probability of the STP exceeding 1, but up to 70% probability of the SCP exceeding 1 by 1800 UTC. It was noted that a 10% probability of the STP exceeding 1 can be a significant signal, given the number of terms in the composite calculation.

The operational NAM indicated that low clouds would likely prevail over SE VA at 1800 UTC, and SREF probability graphics indicated a 90% probability that LCL heights would be less than 750 m AGL across the region. Thompson et al. 2003 determined that LCL heights below roughly 1000 m AGL were meteorologically significant for discriminating between significantly tornadic and nontornadic supercells. Thompson et al. (2003) also found that 0-1 km SRH discriminated strongly between supercells that produced F2-F5 tornadoes and nontornadic supercells. SREF Probability forecasts of low LCL heights in combination with a consistent source of boundary layer moisture, significant 0-1 km SRH, and a likelihood of SCP>1 highlighted a potential for supercells (and possibly a strong tornado) across SE VA during the afternoon of 28 April.

Standardized climate anomaly forecasts indicated a potential for above normal PW values paired with a significant low-level jet over SE VA on 28 April. The strong low-level winds contributed to EBS values of 40 kts, which increased the 0-1 km SRH and enhanced the potential for supercell storms.

Kain et al. (2008) found that the UH diagnostic effectively highlights geographic areas and environmental conditions that favor supercell development. Consequently, high resolution model output from the convection allowing NCEP NMM WRF included SRF and UH, which together substantiated a potential for supercells ahead of bowing line segments across SE VA by 1800 UTC. Although the UH magnitudes were less impressive than UH values typically associated with supercells across the southern Plains, the UH in this study was coincident with SRF-generated cells traversing the area, which increases the confidence that the model was generating supercells across SE VA. Perhaps an alternative form of the UH calculation with a shallower more surface based integration might have worked better with the SE VA storms (Jack Kain, personal communication).

Finally, mesoanalysis graphics from the RUC indicated a SCP > 4 across SE VA, a FLSTP of at least 1, MUCAPE ranging from 1000-1500 J kg^{-1}, and EBS

magnitudes of 40-45 kts across SE VA at 1800 UTC. Especially noteworthy, the MUCAPE values were significantly greater than the forecasts. Given the previously discussed model output, the mesoanalysis graphics substantiated earlier model forecasts for supercells and highlighted a greater-than-forecast potential for tornadoes.

This study demonstrated that the complementary advantages of SREF probability forecasts, post processed convection allowing deterministic model output, and standardized climate anomalies can collectively contribute to a more informative severe weather forecast while providing greater situational awareness for a potentially high impact event.

7. ACKNOWLEDGEMENTS

The authors wish to thank Jon Davies for allowing us to use discussion points from his Severe Weather Notes Blog. We also wish to acknowledge Jack Kain for sharing information related to his current research stemming from the HWT. We are grateful for a timely and productive review from Dave Radell, Easter Region Scientific Services Division.

8. REFERENCES

Benjamin, S. G., K. J. Brundage, and L. L. Morone, 1994a: The Rapid Update Cycle. Part I: Analysis/model description. Technical Procedures Bulletin No.~416, NOAA/NWS, 16 pp.

Bothwell, P. D., J. A. Hart, and R. L. Thompson, 2002: An integrated three-dimensional objective analysis scheme in use at the Storm Prediction Center. *Preprints, 21st Conf. on Severe Local Storms*, San Antonio, TX, Amer. Meteor. Soc., 117-120.

Du, J., J. McQueen, G. DiMego, Z. Toth, D. Jovic, B. Zhou, and H. Chuang, 2006: New Dimension of NCEP Short-Range Ensemble Forecasting (SREF) System: Inclusion of WRF embers, Preprint, WMO Expert Team Meeting on Ensemble Prediction System, Exeter, UK, Feb. 6-10, 2006, 5 pages

Edwards, R., and R.L. Thompson, 2000: RUC-2 Supercell Proximity Soundings, Part II: An Independent Assessment of Supercell Forecast Parameters. *Preprints, 20th Conf. Severe Local Storms*, Orlando FL

Grumm, R.H and Hart, R 2001: Standardized Climatological anomalies applied to significant cold season weather events. *Wea. Forecasting*, **16**, 736-754.

Hart, J.A. and W.D. Korotky, 1991: The SHARP Workstation -v1.50 A Skew T/Hodograph Analysis and Research Program for the IBM and Compatible PC. User's Manual. NOAA/NWS Forecast Office, Charleston, WV, 62 pp.

Hart, R, and R.H. Grumm 2001: Using standardized climatological anomalies to rank synoptic-scale events objectively. *Mon. Wea. Rev*., **129**, 2426-2442.

Kain, J. S., S. J. Weiss, D. R. Bright, M. E. Baldwin, J. J. Levit, G. W. Carbin, C. S. Schwartz, M. L. Weisman, K. K. Droegemeier, D. B. Weber, K. W. Thomas, 2008: Some practical considerations regarding horizontal resolution in the first generation of operational convection-allowing NWP. *Wea. Forecasting*, **23**, 931-952.

Kalnay and coauthors: 1996: The NCEP/NCAR 40-year re-analysis project. *Bull. Amer. Meteor. Soc.,* **77**, 437-471.

Koch, S. E., B. Ferrier, M. Stolinga, E. Szoke, S. J. Weiss, and J. S. Kain, 2005: The use of simulated radar reflectivity fields in the diagnosis of mesoscale phenomena from high-resolution WRF model forecasts. *Preprints, 11th Conference on Mesoscale Processes*, Albuquerque, NM, Amer. Meteor. Soc., CD-ROM, J4J.7

Korotky, W. D., Using ensemble probability forecasts and high resolution models to identify severe weather threats. *Preprints, 23rd Conf on Severe Local Storms*, St. Louis MO, Amer. Meteor. Soc.

Markowski, P.M., J.M. Straka, and E.N. Rasmussen, 2002: Direct Surface Thermodynamic Observations within the Rear-Flank Downdrafts of Nontornadic and Tornadic Supercells. *Mon. Wea. Rev.*, **130**, 1692–1721.

Roebber, P.J., D.M. Schultz, B.A. Colle, and D.J. Stensrud, 2004: Toward Improved Prediction: High-Resolution and Ensemble Modeling Systems in Operations. *Wea. Forecasting*, **19**, 936–949.

Thompson, R.L., C.M. Mead, and R. Edwards, 2007: Effective Storm-Relative Helicity and Bulk Shear in Supercell Thunderstorm Environments. *Wea. Forecasting*, **22**, 102–115.

Thompson, R.L., C.M. Mead, and R. Edwards, 2004: Effective bulk shear in supercell thunderstorm environments. *Preprints*, *22nd Conf. on Severe Local Storms*, Hyannis MA.

Thompson, R.L., R. Edwards, J.A. Hart, K.L. Elmore, and P. Markowski, 2003: Close Proximity Soundings within Supercell Environments Obtained from the Rapid Update Cycle. *Wea. Forecasting*, **18**, 1243–1261.

Weiss, S.J., D.R. Bright, J.S. Kain, J.J. Levit, M.E. Pyle, Z.I. Janjic, B.S. Ferrier, and J. Du, 2006: Complementary Use of Short-range Ensemble and 4.5 KM WRF-NMM Model Guidance for Severe Weather Forecasting at the Storm Prediction Center. *Preprints, 23rd Conf. Severe Local Storms*, St. Louis MO, Amer. Meteor. Soc.